Journal of Clinical Cases and Reports

ISSN: 2582-0435 **Clinical Research** | Vol 4 Iss 1

In Vivo Biomechanical Analysis of Human Tendon Using Vibrational Optical Coherence Tomography: Preliminary Results

Frederick H Silver*, Istvan Horvath, Nikita Kelkar, Tanmay Deshmukh and Ruchit Shah

OptoVibronex, LLC, Allentown, Pa, USA

Correspondence should be addressed to Frederick H Silver, fhsilverfh@yahoo.com; fhsilver@hotmail.com

Received: December 20, 2019; Accepted: January 01, 2020; Published: January 08, 2020

ABSTRACT

The mechanical properties of tendons measured *in vitro* have been reported previously. However, attempts to measure the elastic modulus *in vivo* have been limited to estimates of the properties based on indirect methods. The purpose of this paper is to introduce the use of vibrational optical coherence tomography (VOCT) to measure the resonant frequency and modulus of patellar and Achilles tendons.

VOCT is a non-invasive and non-destructive method that uses infrared light and audible sound to create a displacement of skin. This displacement of skin subsequently leads to vibrations of subcutaneous tissues as deep as 4 cm. The result of these vibrations is a measured spectrum of resonant frequencies of all vibrating tissues that are recoded using VOCT. The measured resonant frequencies are converted into bulk modulus values using a calibration curve.

Results reported in this paper indicate that the cutaneous resonant frequency reflecting the behavior of the patellar and Achilles tendons is about 440 Hz. The calculated *in vivo* strain is about 2.5% based on reported stress-strain testing *in vitro* and the calculated elastic modulus is about 34 MPa for both tendons. Using VOCT, elastic modulus measurements made *in vivo* provide insight into the physiology and pathology of tendon as well as the mechanisms of injury. In addition, alterations in tendon structure and function due to genetic mutations, mechanical injury, and aging effects can be evaluated. Measurements using VOCT can also provide a quantitative basis for evaluating treatment efficacies for tendon injuries.

Keywords

Tendon; Mechanical properties; Elastic modulus; Vibrational optical coherence tomography; Skin; Resonant frequency

1. INTRODUCTION

Tendon and ligaments are multi-component elements that cyclically transmit force and store elastic energy in the absence of permanent changes in length [1-3]. Elastic energy storage in tendons in the legs and feet of many animals is an important mechanism that saves substantial quantities of muscular energy [4-6]. Extensive research on the structure and properties of tendons and ligaments has led to a detailed model of these tissues [3,7-11]. The major

Citation: Frederick H Silver, In Vivo Biomechanical Analysis of Human Tendon Using Vibrational Optical Coherence Tomography: Preliminary Results. J Clin Cases Rep 4(1): 12-19.

component of tendon is the collagen fibril that is made up of quarter-staggered collagen molecules packed into a quasi-hexagonal packing pattern [3]. The fibrils are in turn packed into fibril bundles that make up the fascicular units within the tendon [3].

The mechanical properties of model tendons composed of reconstituted type I collagen fibers have been studied extensively [12-15]. The modulus and strength of the fibers requires the presence of end-to-end crosslinks between collagen molecules in the collagen quarter staggered packing pattern [13-15]. In the absence of crosslinks, self-assembled collagen fibers behave in a predominantly viscous fashion and lack the ability to store energy and return to their original length after unloading [13-15]. However, crosslinked collagen fibers can store about 70% of the applied energy during deformation [13-16] and this energy can be transmitted and dissipated without causing tendon failure [3,13-16]. Therefore the ability of tendon to store, transmit and dissipate elastic energy required for locomotion is an important property of these tissues [3]. The results of one study suggest that measurements of the elastic modulus of tendons can be used to predict the ultimate tensile strength for diseased or injured tendons [17]. Therefore, it would be useful to non-invasively measure the elastic modulus of tendons *in vivo* in order to analyze the pathophysiology of tendon injury.

Recently, we have developed a method to non-invasively image and measure the mechanical properties of human epidermis and dermis *in vivo* using a combination of optical coherence tomography and vibrational analysis [18-25]. The technique is termed vibrational optical coherence tomography (VOCT) and provides an image that can be quantitatively analyzed by scanning the pixel intensity [18-25]. Using VOCT, the resonant frequency and modulus (stiffness) of both the cellular and macromolecular components can be measured. The stiffness of the epidermis and dermis can then be calculated from the resonant frequency and tissue thickness [18-25]. These measurements have been used to identify the type of skin lesions and follow wound healing and scarring of skin [18-28]. The image depth using optical coherence tomography is limited to about 2 mm, however, when a sound wave is applied to the skin the resonant frequencies of the reflected sound waves from internal tissues as deep as 4 cm can be measured on the surface of the skin. Using VOCT it is possible to detect the resonant frequency and calculate the average bulk modulus of underlying tissue structures based on the resonant frequencies observed from the skin vibrational spectrum.

The purpose of this paper is to present preliminary *in vivo* measurements of the resonant frequency and modulus of patellar and Achilles tendons. The results of these studies suggest that the average bulk elastic modulus of human tendons can be measured *in vivo* using VOCT.

2. METHODS

Vibrational optical coherence tomography (VOCT) and vibrational analysis *in vivo*

VOCT is a non-invasive and non-destructive method that uses infrared light and audible sound to create a displacement of skin [18-28]. The displacement of the skin causes vibrations in subcutaneous tissues that are reflected back to the skin. The result is a spectrum of resonant frequencies that are recorded by measuring the displacement of the skin as a function of frequency. The measured resonant frequencies are converted into modulus values using a calibration curve developed based on *in vitro* uniaxial mechanical tensile testing [18-28].

Experimentally, the VOCT hand piece is placed in a stand, as described previously [18-28], and then the infrared light is focused on the area of skin above the patellar or Achilles tendon. An OCT scanning image of the skin is obtained to insure that the epidermis and dermis are normal [18-25]. Cutaneous displacement is generated using audible sound by placing a blue tooth speaker near the skin as discussed

previously [18-28]. The spectral-domain optical coherence tomography (SD-OCT) system uses a fiber-coupled superluminescent diode light source with an 840 nm center wavelength and 100 nm bandwidth (full-width at half maximum) [18-28]. Although the infrared light only penetrates about 0.5 mm to 1 mm into the skin the audible sound will penetrate about 4.0 cm through the subcutaneous tissues.

Tests were conducted on 15 volunteers with ages ranging from 24-70-years old after informed consent was obtained. All studies were conducted at 75°F and 40% to 50% relative humidity. A frequency generating app was downloaded onto the I5 processor within the OCT device. This app was capable of driving the speaker between 30 Hz and 20,000 Hz [15-28]. The speaker was placed in several locations near skin on the knee and back of ankle but was not in contact with the skin. During *in vivo* measurements, no sensation of the light or sound is felt impinging on the skin.

The resonant frequency of each sample is determined by measuring the displacement of the skin resulting from sinusoidal driving frequencies ranging from 30 Hz to 600 Hz, in steps of 10 Hz. The peak frequency (the resonant frequency), f_n, is defined as the frequency at which the displacement is maximized as discussed previously [15-28]. The moduli of skin and tendons are calculated from measurements of the resonant frequency, skin thickness, and images of the skin. Moduli are then obtained from a calibration curve that relates resonant frequency and thickness to modulus values (Figure 1). The moduli of the samples are obtained by determination of the resonant frequency from a plot of weighted displacement versus frequency (Figure 2) and then by dividing by the skin thickness obtained from the OCT image. The skin thickness is used since vibrations from the subcutaneous tissues give rise to vibrations on the surface of skin characteristic of each tissue vibrating. The weighted displacement versus frequency curve becomes a mechanical spectrum generated by the components of the tissues that vibrate [18-28]. Weighted displacement is normalized by dividing by the displacement of the speaker in the absence of the sample. The bulk modulus is obtained from the measured resonant frequency and sample thickness and using Figure 1.

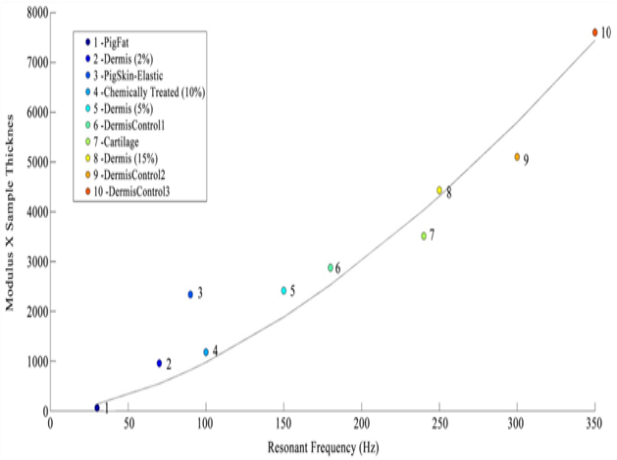

Figure 1: Calibration curve showing relationship between modulus times the sample thickness versus the resonant frequency determined *in vitro* from tensile and vibrational measurements made on the same material at the same time.

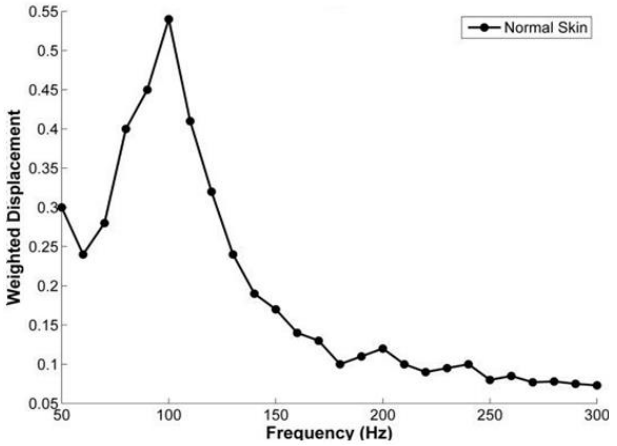

Figure 2: Weighted displacement versus frequency for normal skin of the hand. Note the resonant frequency of the cellular epidermis is seeing at frequencies between 50 Hz and 70 Hz while that of collagen of the dermis has a resonant frequency between 100 Hz and 140 Hz (Table 1).

The original grayscale OCT images of skin are pseudo color-coded based on the pixel intensities to provide better images of the tissue components as describe previously [18-25]. The enhanced OCT images use darker colored

(blue and purple) regions to reflect lower pixel intensities while the lighter (yellowish) regions reflect higher pixel intensity regions (Figure 3).

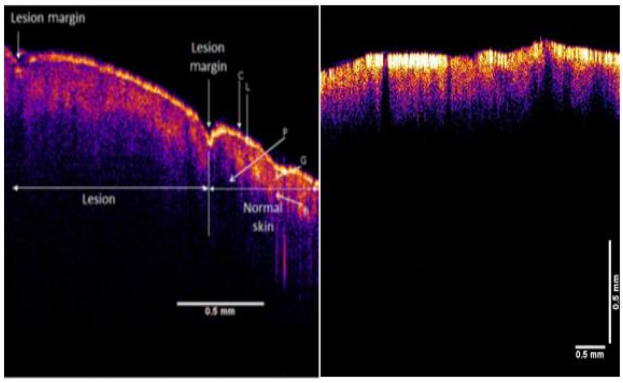

Figure 3: Enhanced OCT image of normal skin from the hand (Left) showing the different layers of the epidermis including the stratum corneum (C), lamina lucidum (L), papillary dermis (P) stratum basale (B) and the stratum granulosum (G). Skin on left hand side of the normal skin is a scar. The skin above the patellar tendon is shown on the right. Note the black vertical lines are from the hair follicles that protrude through the skin.

3. RESULTS

Images, resonant frequencies and moduli were measured for skin, patellar tendon and Achilles tendons on 15 subjects. A typical enhanced OCT image of the skin above the tendons is shown in Figure 3.This image, resonant frequency and modulus data indicate that the cutaneous measurements are similar to measurements reported previously [18-28] (Table 1). The skin shows the cellular layers of the epidermis as well as the collagen in the papillary dermis. Figure 2 is a weighted displacement versus frequency curve for normal skin away from the tendon illustrating that there is a small cellular peak at about 50 Hz - 70 Hz and a collagen peak at about 100 Hz - 140 Hz. The resonant frequencies and moduli of skin and the tendons measured are listed in Table 1. In the case of the tendons, the cellular and collagen peaks of the skin are overshadowed by the large tendon peak at 440 Hz. For patellar tendon additional peaks are observed at about 300 Hz and 350 Hz. These peaks likely arise from the synovial covering and/or fat pad on top of the tendon; however, further measurements are needed on isolated tissues to confirm this hypothesis The peak observed at about 100 Hz in Figure 4 represents that of the skin as previously reported: that observed at a frequency of 440 Hz is that of the patellar tendon.

Both patellar and Achilles tendons were found to have resonant frequencies of about 440 Hz and moduli of about 34 MPa (Table 1). Normal skin above the patellar tendon was found to have a modulus of 2 MPa to 3 MPa similar to that of skin reported previously [18-28].

LaCroix et al. [17] have published a study of ultimate tensile strength versus elastic modulus determine from the slope of the tensile stress-strain curve. They concluded that a single plot of this data for tendons from humans and animals has slope of 0.0932 and a strain at failure 9.7%. Using this relationship and the modulus calculated from vibrational studies 34 MPa, then the calculated value of UTS for these tissues is 365 MPa.

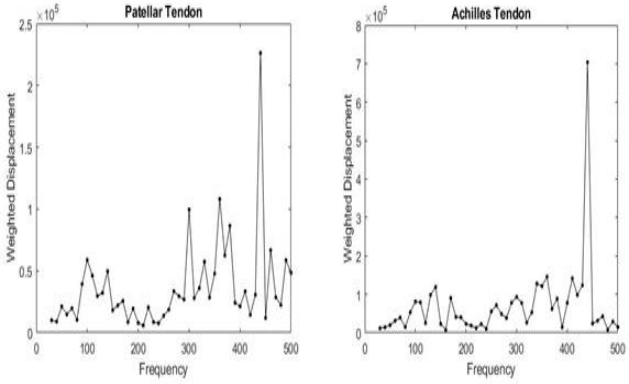

Figure 4: Weighted displacement versus frequency of skin above the patellar tendon (left) and Achilles (right). The patellar tendon exhibits a collagen peak at about 100 Hz and peaks at 300 Hz, 350 Hz, and 440 Hz. The Achilles tendon has a large peak at 440 Hz.

The modulus as a function of strain for patellar tendon calculated from the data reported by Innocenti et al. [29] is shown in Figure 5. Using Figure 5 and the experimental modulus 34 MPa, see Table 1, the value of the *in vivo* strain appears to be about 2.5% based *in vitro* testing. This

strain value is consistent with the patellar tendon operating at the intersection between the low and high modulus regions *in vivo*.

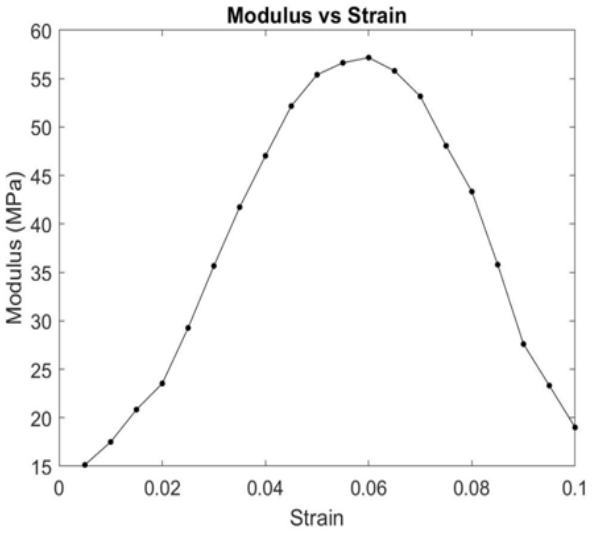

Figure 5: Modulus as a function of strain calculated for patellar tendon from Innocenti et al. [29]. Note patellar tendon appears to operate at the beginning of the linear region of the stress-strain curve. The *in vivo* strain for patellar tendon in a non-weight bearing state appears about 2.5%.

4. DISCUSSION

The ability of tendon to bear loads, store, transmit and dissipate elastic energy depends on the structure and stability of collagen molecules, fibrils, fibril bundles and fascicles [1-11]. The energy storage capability has been modelled to involve the flexible regions in the collagen triple helix [30-32]. Their ability to undergo reversible deformations is driven by free energy considerations involving flexible Gly-X-Y sequences [32].

An additional requirement for energy storage is the presence of end-to-end crosslinks between neighboring collagen molecules that form a continuous stress bearing network [3]. Without these crosslinks deformation of collagen fibers is predominantly a viscous event leading to permanent deformation of the collagen fibers and premature fiber failure [3,8,9]. The decrease in the modulus of patellar tendon (Figure 5) prior to failure reflects defibrillation of the collagen fibers that lowers the tendon stiffness [3,9].

Sample	Resonant Frequency (Hz)			Moduli (MPa)			Number of Observations
	Cellular	Collagen		Cellular	Collagen		
Skin	50-70	100-140	NA	1.17{0.25}	2.94{0.89}	NA	15
Patellar Tendon	NA	100-140	440	NA	2.46{0.57}	33.79{4.62}	4
Achilles Tendon	NA	NA	440	NA	NA	33.99{5.98}	4

Table 1: Moduli values for cellular and collagen components of skin and tendon measured using OCT and vibrational analysis. Note that the vibrational spectrum of skin and subcutaneous tissues are all seen in Figure 4. In patellar tendon, the peak for skin collagen is between 100 Hz and 140 Hz similar to that seen for the hand. The modulus for skin collagen is between 2 MPa and 3 MPa. The peak seen at 440 Hz has a modulus of about 34 MPa for both the patellar and Achilles tendon. The collagen modulus for patellar tendon 34 MPa, occurs in a tensile stress-strain curve at a strain of about 2.5%. The resonant frequencies are given in Hz and the moduli in MPa. Values for the resonant frequency for the cellular component of skin over the patellar and Achilles tendon could not be calculated because the peaks were too small (NA). The skin collagen peak over the Achilles tendon was also too small to measure. The standard deviation of the moduli values is listed in parentheses { }.

In this study we present data to evaluate the *in vivo* stiffness of human patellar and Achilles tendons. Using a new technique, termed vibrational optical coherence tomography, it is possible to measure the frequencies at which the displacement of the major tissue components are maximized [18-28]. The modulus is then calculated from a calibration curve developed using uniaxial tensile data obtained *in vitro* [25-28]. Our results suggest that the modulus of patellar and Achilles tendons is about 34 MPa, and the calculated *in vivo* strain based on *in vitro* testing data [29] is about 2.5%.

These results suggest that under normal physiological

conditions both tendons operate at the beginning of the linear region of the stress-strain curve. This suggests that the crimp seen morphologically in tendons during tissue dissection may not exist *in vivo*. The crimp maybe removed by the tendon pretension required to maintain normal tissue metabolism through mechanotransduction [3,21].

The ability to measure the elastic modulus non-invasively and non-destructively *in vivo* may provide the ability to link elastic modulus measurements, predicted tendon strength, and tendon pathology. These measurements are useful to understand tendon failure and injury. Tissue analysis using VOCT would add insight into the mechanisms of injury as well alterations in tendon structure and function due to genetic mutations, mechanical injury, and aging effects. It would also provide a quantitative basis for evaluating treatment efficacies for tendon injuries.

5. CONCLUSION

Preliminary measurements of the elastic modulus of patellar and Achilles tendons *in vivo* are reported using a new technique, vibrational optical coherence tomography (VOCT). The measured modulus *in vivo* of patellar and Achilles tendons with no load bearing is 34 MPa. Using this modulus value and based on *in vitro* stress-strain curves for patellar tendons, it is concluded that the estimated strain *in vivo* is about 2.5%. This value corresponds to measurements found *in vitro* at the beginning of the linear stress-strain region.

Use of VOCT to measure the elastic modulus of tendons *in vivo* may help clinicians and researchers better understand failure and injury to this tissue. Such an analysis would add insight into the mechanisms of injury as well alterations in tendon structure and function due to genetic mutations, mechanical injury, and aging effects. It also would provide a quantitative basis for evaluating treatment efficacies for tendon injuries.

REFERENCES

1. Kato YP, Christiansen DL, Hahn RA, et al. (1989) Mechanical properties of collagen fibres: A comparison of reconstituted and rat tail tendon fibres. Biomaterials 10(1): 38-42.
2. McBride DJ, Trelstad RL, Silver FH (1988) Structural and mechanical assessment of developing chick tendon. International Journal of Biological Macromolecules 10(4): 194-200.
3. Silver FH, Freeman JW, Seehra GP (2003) Collagen self-assembly and the development of tendon mechanical properties. Journal of Biomechanics 36(10): 1529-1553.
4. Alexander RM (1983) Animal mechanics 2nd (Edn.). Blackwell Scientific, Oxford, UK
5. Alexander RM (1984) Elastic energy stores in running vertebrates. Integrative and Comparative Biology 24(1): 85-94.
6. Shadwick RE (1990) Elastic energy storage in tendons: Mechanical differences related to function and age. Journal of Applied Physiology 68(3): 1033-1040.
7. Elliott DH (1965) Structure and function of mammalian tendon. Biological Reviews of the Cambridge Philosophical Society 40: 392-421.
8. Diamant J, Keller A, Baer E, et al. (1972) Collagen ultrastructure and its relationship to mechanical properties as a function of ageing. Proceedings of the Royal Society of London Series B 180(1060): 293-315.
9. Torp S, Baer E, Friedman B (1975) Effects of age and of mechanical deformation on the ultrastructure of tendon. Structure of Fibrous Biopolymers 26: 223-250.
10. Goldstein JD, Tria AJ, Zawadsky JP, et al. (1989) Development of a reconstituted collagen tendon prosthesis. A preliminary implantation study. Journal Bone and Joint Surgery 71(8): 1183-1191.

11. Yahia LH, Drouin G (1989) Microscopical investigation of canine anterior cruciate ligament and patellar tendon: Collagen fascicle morphology and architecture. Journal of Orthopaedic Research 7(2): 243-251.
12. Danielsen CC (1981) Mechanical properties of reconstituted collagen fibrils: A study on reconstitution methodology and influence of in vitro maturation. Connective Tissue Research 9(1): 51-57.
13. Christiansen DL, Huang EK, Silver FH (2000) Assembly of type I collagen: Fusion of fibril subunits and the influence of fibril diameter on mechanical properties. Matrix Biology 19(5): 409-420.
14. Silver FH, Christiansen DL, Snowhill PB, et al. (2001) Transition from viscous to elastic-dependency of mechanical properties of self-assembled collagen fibers. Journal of Polymer Science 7(1): 134-142.
15. Silver FH, Ebrahimi A, Snowhill PB (2002) Viscoelastic properties of self-assembled type I collagen fibers: Molecular basis of elastic and viscous behaviors. Connective Tissue Research 43(4): 569-580.
16. Dunn MG, Silver FH (1983) Viscoelastic behavior of human connective tissues: Relative contribution of viscous and elastic components. Connective Tissue Research 12(1): 59-70.
17. LaCroix AS, Duenwald-Kuehl SE, Lakes RS, et al. (1985) Relationship between tendon stiffness and failure: A metaanalysis. Journal of Applied Physiology 115(1): 43-51.
18. Shah RG, Pierce MC, Silver FH (2017) Morphomechanics of dermis-A method for non-destructive testing of collagenous tissues. Skin Research and Technology 23(3): 399-406.
19. Shah R, Pierce MC, Silver FH (2017) A method for nondestructive mechanical testing of tissues and implants. Journal of Biomedical Materials Research Part A 105(1): 15-22.
20. Shah RG, DeVore D, Silver FH (2018) Biomechanical analysis of decellularized dermis and skin: Initial in vivo observations using optical cohesion tomography and vibrational analysis. Journal of Biomedical Materials Research Part A 106(5): 1421-1427.
21. Silver FH (2017) A matter of gravity-mechanotransduction: How mechanical forces influence biological materials. Material Science & Engineering International Journal 1(2): 66-68.
22. Silver FH, Silver LL (2017) Non-invasive visco-elastic behavior of human skin and decellularized dermis using vibrational OCT. Dermatology Clinics and Research 3(3): 174-179.
23. Silver FH, DeVore D, Shah R (2017) Biochemical, biophysical and mechanical characterization of decellularized dermal implants. Material Sciences and Applications 8(12): 873-888.
24. Silver FH, and Silver LL (2018) Use of vibrational optical coherence tomography in dermatology. Archives of Dermatology and Skin Care 1(2): 3-8.
25. Silver FH, Shah RG, Benedetto D, et al. (2019) Virtual biopsy and physical characterization of tissues, biofilms, implants and viscoelastic liquids using vibrational optical coherence tomography. World Journal Mechanics 9(1): 1-16.
26. Silver FH, Shah RG, Richard M, et al. (2019) Comparative "virtual biopsies" of normal skin and skin lesions using vibrational optical coherence tomography. Skin Research and Technology 25(5): 743-749.
27. Silver, FH, Shah, RG, Richard M, et al. (2019) Comparison of the virtual biopsies of a nodular basal cell carcinoma and an actinic keratosis: Morphological, cellular and collagen analyses. Advances in Tissue Engineering and Regenerative Medicine 5(2): 61-66.
28. Silver, FH, Shah, RG, Richard M, et al. (2019) Use of vibrational optical coherence tomography to image and characterize a squamous cell carcinoma. Journal of Dermatology Research and Therapy 5(1): 067.

29. Innocenti B, Larrieu JC, Lambert P (2018) Automatic characterization of soft tissues material properties during mechanical tests. Muscle, Ligaments and Tendons Journal 7(4): 529-537.
30. Paterlini MG, Némethy G, Scheraga HA (1995) The energy of formation of internal loops in triple-helical collagen polypeptides. Biopolymers 35(6):607-619.
31. Hofmann H, Voss T, Kühn K, et al. (1984) Localization of flexible sites in thread-like molecules from electron micrographs: comparison of interstitial, basement membrane and intima collagens. Journal of Molecular Biology 172(3): 325-343.
32. Silver FH, Horvath I, Foran DJ (2002) Mechanical implications of the domain structure of fiber-forming collagens: comparison of the molecular and fibrillar flexibilities of the alpha1-chains found in types I-III collagen. Journal of Theoretical Biology 216(2): 243-254.